Adaptive support domain implementation on the Moving Least Squares approximation for Mfree methods applied on elliptic and parabolic PDE problems using strong-form description

G. C. Bourantas[1], E. D. Skouras[2,3*], and G. C. Nikiforidis[1]

[*]*Correspondence:* Eugene.Skouras@iceht.forth.gr

Abstract The extent of application of meshfree methods based on point collocation (PC) techniques with adaptive support domain for strong form Partial Differential Equations (PDE) is investigated. The basis functions are constructed using the Moving Least Square (MLS) approximation. The weak-form description of PDEs is used in most MLS methods to circumvent problems related to the increased level of resolution necessary near natural (Neumann) boundary conditions (BCs), dislocations, or regions of steep gradients. Alternatively, one can adopt Radial Basis Function (RBF) approximation on the strong-form of PDEs using meshless PC methods, due to the delta function behavior (exact solution on nodes). The present approach is one of the few successful attempts of using MLS approximation [Atluri, Liu, and Han (2006), Han, Liu, Rajendran and Atluri (2006), Atluri and Liu (2006)] instead of RBF approximation for the meshless PC method using strong-form description. To increase the accuracy of the MLS interpolation method and its robustness in problems with natural BCs, a suitable support domain should be chosen in order to ensure an optimized area of coverage for interpolation. To this end, the basis functions are constructed using two different approaches, pertinent to the dimension of the support domain. On one hand, a compact form for the support domain is retained by keeping its radius constant. On the other hand, one can control the number of neighboring nodes as the support domain of each point. The results show that some inaccuracies are present near the boundaries using the first approach, due to the limited number of nodes belonging to the support domain, which results in failed matrix inversion. Instead, the second approach offers capability for fully matrix inversion under many (if not all) circumstances, resulting in basis functions of increased accuracy and robustness. This PC method, applied along with an intelligent adaptive refinement, is demonstrated for elliptic and for parabolic PDEs, related to many flow and mass transfer problems.

Keywords: Meshless Methods; Point Collocation Methods; Strong Form description; MLS; Adaptive Support Domain;

1 Introduction

In recent years, research on meshless (meshfree) methods has made significant progress in science and engineering, particularly in the area of computational mechanics. The finite element method (FEM), which has been the most frequently used numerical method in engineering during the past 30 years, has faced inefficiencies in further development and optimization. More specifically, the lack of a robust and efficient 3D mesh generator makes the calculation of a general solution of 3D problems a difficult task. Furthermore, mesh-based methods are not suited for problems having large deformations [Liu (2002)]. Thus, much attention has been focused on the development of meshes methods, such as the Smooth Particle Hydrodynamics (SPH) [Gingold and Monaghan (1977)], the Diffuse Element Method (DEM) [Nayroles, Touzot and Villon (1992)], the Element Free Galerkin Method (EFG) [Belytschko, Lu and Gu (1994)], the Reproducing Kernel Particle Method (RKPM) [Liu, Chen, Jun, Chen Belytschko, Pan, Uras and Chang (1996)], the Finite Point Method (FP) [Onate, Idelsohn, Zienkiewicz and Taylor (1996)], the hp Clouds Method (HP) [Liszka, Duarte and Tworzydlo (1996)], the Meshless Local Petrov-Galerkin method (MLPG) [Atluri and Zhu (1998), Atluri (2004), Atluri and Shen (2002)], as well as the Local Boundary Integral Equation method (LBIE) [Atluri, Sladek, Sladek and Zhu (2000)].

Two methods of discretization, namely the collocation method and the Galerkin method, have been dominant in existing meshless methods. Both methods are produced by the implementation of the weighted residuals method. The latter is one of the most general procedures for solving numerically Partial Differential Equations (PDEs). Collocation method usually solves the strong form of the Partial Differential Equations, while the Galerkin method

[1] Department of Medical Physics, School of Medicine, University of Patras, GR 26500, Rion, Greece.

[2] Department of Chemical Engineering, University of Patras, GR 26500, Rion, Greece.

[3] Institute of Chemical Engineering and High Temperature Chemical Processes - Foundation for Research and Technology, P.O. Box 1414, GR-26504, Patras, Greece.

deals with the weak formulation. At the first case, the solution obtained is commonly referred to as the strong solution, while the second as the weak. One of the most challenging tasks in the solution of partial differential equations is the selection of the strong or the weak formulation. The strong formulation is usually easy to implement, however it suffers from certain inaccuracies when singularities exist at the boundaries (Neumann boundary conditions). The weak formulation instead, has some complications as far as the implementation issues are concerned, however it is often stated as to be more stable when dealing with natural boundary conditions.

In general, a strong solution is always a full solution of the weak formulation; however a weak solution is not always a complete strong one. Numerical methods that are dealing with integration, such as finite element method, boundary element equation method, Element Free Galerkin (EFG) meshless method, and meshless local Petrov-Galerkin (MLPG) method, all provide a weak solution. Instead, pointwise collocation methods result mainly in strong solutions. A crucial point is whenever to use a strong or a weak form of the partial differential equation. From mathematical point of view, the answer to that question is that depends on the boundary conditions and the selection of the trial functions. For the first case, when the geometry of a domain Ω has irregularities, such as incoming corners, even if the data functions f^{Ω} and $f^{\partial\Omega}$ are smooth, there may be singularity of the approximation function at the boundary. Concerning the second case, non-smooth data at certain boundary points lead to inaccuracies for the solution in contrast to the weak formulation that uses a weighted average values for the boundary data. Things are different when applications in science and engineering insist on distributional data where the weak forms are unavoidable. Many of the strong form techniques can be transferred to weak forms. The meshless local Petrov-Galerkin (MLPG) method is a good example of a weak meshless technique with plenty of successful applications in engineering. However, it is weak and unsymmetric, and not until recently a solid theoretical formation was given [Schaback (2007)].

In the present work we purposely used the strong form meshless collocation method for solving two-dimensional partial differential equations of the elliptic and the parabolic type, as well. The authors insist on strong form description, as it can provide point-wise accurate solutions for time dependent problems (parabolic), as the pulsatile flows in constrictions (blood flow in aneurisms and stenoses, [Kagadis**,** Skouras, Bourantas, Paraskeva, Katsanos, Karnabatidis and Nikiforidis (in press)]), but can be particularly useful in multiscale problem when used “in-line” with other, “less” continuum, methods. Such multiscale or interdimentional, coupled methods include mixed Computational Fluid Dynamics (CFD) and Direct Simulation Monte Carlo (DSMC) approaches with Dirichlet-Dirichlet type boundaries [Garcia, Bell, Crutchfield and Alder (1999)], description of particles-liquid-solids interactions, as in porous materials [Burganos, Skouras, Paraskeva, and Payatakes (2001), Skouras Paraskeva, Burganos, and Payatakes (2007)], in gas-liquid interactions (solution-evaporation) and gas-solid interactions (sorption-catalysis) [Navascués, Skouras, Nikolakis, Burganos, Tellez and Coronas (in press)]. Meshless methods can be used to obtain diffusivities, permeabilities, sorption constants and other transport and separation parameters from their microscopic origins in compressible and non-continuum flows [Michalis, Kalarakis, Skouras and Burganos (2008)], in microfluidic filters [Aktas and Aluru (2002)], and in vacuum technology [Garcia, Bell, Crutchfield and Alder (1999)].

The Moving Least Square method for the approximation of the field variable is applied. An exponential weight function is used for the construction of the approximated function, which is applied on a constant number of support nodes, instead of a constant node density support domain. An automated procedure for node refinement is proposed, based on a strong form error finding approach. More specifically, nodes on which the error of the calculated field property is above a user-defined threshold are extracted and surrounded by additional nodes, which are added with a predefined formulation; overall, an approach which obtains convergence for the solution of the governing equations. The refining method reduces the computational cost and time, while leading to more accurate and significantly stable results. The procedure is fully automated and robust. Finally, a two-dimensional Stokes fluid flow problem is presented and the results are compared with the results obtained with the commercial package ANSYS CFX.

The weighted residual method provides a flexible mathematical framework for the construction of a variety of numerical solution schemes for the differential equations arising in the field of both science and engineering. Its application, in conjunction with the Moving Least Square (MLS) approximation method, yields powerful solution algorithms for the governing equations.

Considering a problem governed by a differential equation

$$L[u(x)] = f \quad \text{in } \Omega, \tag{1}$$

with Neumann boundary conditions

$$B[u(x)] = t \quad \text{on } \Gamma_t, \tag{2}$$

and Dirichlet boundary conditions

$$u - u_p = 0 \quad \text{on } \Gamma_u, \tag{3}$$

studied over the domain Ω, which is a sufficiently smoothed, closed, and surrounded by a continuous boundary $\partial\Omega = \Gamma_u \cup \Gamma_t$. In equations (1)-(3), L and B are the

corresponding differential operators, $u(x)$ is the dependent variable of the problem (a function of independent spatial variables), u_p is the prescribed value of the unknown function over the boundary Γ_u, while f and t are the forces and the source or sink terms acting over the domain Ω and the boundary Γ_t respectively. In the absence of an exact analytical solution for equation (1) one may seek to represent the field variable $u(x)$ approximately as

$$u^h(x) = \sum_{i=1}^{m} a_i \Phi_i \tag{4}$$

where a_i are a set of coefficients (constants), whereas Φ_i represents a set of geometrical functions, usually called basis functions.

Accuracy and convergence of the defined approximation will depend on the selected basis functions and (as a rule of thumb) these functions should be chosen in a way that the approximation gradually becomes more accurate as m increases. Substitution of equation (4) into equation (1) gives

$$L\left[u^h(x)\right] - f = R_\Omega \tag{5}$$

where R_Ω is the residual that appears through the insertion of an approximation instead of an exact solution for the unknown function $u(x)$.

The residual R_Ω is a function of position inside Ω. The weighted residual method is based on the minimization of this residual over the entire domain. For this minimization procedure to be achieved the residual is weighted by an appropriate number of position-dependent functions and a summation is carried out. The latter is written

$$\int_\Omega W_j R_\Omega d\Omega = 0 \qquad \text{j=1, 2, 3, . . . m} \tag{6}$$

where W_j are the independent weight functions and $d\Omega$ is an appropriate integration interval. Applying the weighted residual method to the above equations one gets

$$\int_\Omega W_i\left(Lu^h - b\right)d\Omega + \int_{\Gamma_t} W_i\left(Bu^h - t\right)d\Gamma + \int_{\Gamma_u} W_i\left(u^h - u_p\right)d\Gamma = 0 \tag{7}$$

with the weighted functions W_i, W_i, W_i defined in appropriate ways. Theoretically, the above equation should provide a system

$$Ku = f \tag{8}$$

of *m* linear equations to be solved, in order to calculate the coefficients a_i in equation (4).

In cases where $\overline{W}_i \equiv \delta_i$, δ_i being the Dirac delta function, equation (7) can be written:

$$\begin{aligned} Lu_i^h &= b \ ; \qquad i \in \Omega, \\ Bu_j^h &= t \ ; \qquad j \in \Gamma_t, \\ u_k^h &= u_p \ ; \qquad k \in \Gamma_u, \end{aligned} \tag{9}$$

leading to a linear system as the one in equation (8).

2 Moving Least Squares

2.1 Moving Least Square Approximation

Let $u(x)$ be the unknown function of the field variable defined in the domain Ω. The function $u^h(x)$ is the approximation of function $u(x)$ at point x. The field function is defined using the Moving Least Square (MLS) approximation as

$$u^h(x) = \sum_{i=0}^{m} p_i(x) a_i(x) \equiv \mathrm{p}^T(x)\mathrm{a}(x) \tag{10}$$

where *m* is the number of terms of monomials (polynomial basis), and $\mathrm{a}(x)$ is a vector of coefficients given by

$$\mathrm{a}^T(x) = \left\{a_0(x)\ a_1(x) ... a_m(x)\right\} \tag{11}$$

which are functions of x.

Given a set of *n* nodal values, of a field function $u_1, u_2, ..., u_n$, at *n* nodes $x_1, x_2, ..., x_n$ inside the support domain, equation (10) can be used for the calculation of the approximated values of the field function at these nodes:

$$u^h(x, x_i) = p^T(x_i)\mathrm{a}(x) \quad \text{i=1, 2, 3, …, n} \tag{12}$$

The coefficients $\mathrm{a}_i(x)$ are calculated by the minimization of the quadratic functional $J(x)$ given by

$$J(x) = \sum_{i=1}^{n} w(x - x_i)\left\{\sum_{j=1}^{m} p_j(x_i)\mathrm{a}_j(x) - u_i\right\}^2 \tag{13}$$

The minimization conditions requires

$$\frac{\partial J}{\partial a}=0 \tag{14}$$

which results in the following linear equation system:

$$A(x)\mathrm{a}(x)=B(x)U_s \tag{15a}$$

where **A** is the (weighted) moment matrix, expressed by

$$A(x)=\sum_{i=1}^{n}\overline{W}_i(x)\mathrm{p}(x)\mathrm{p}^{\mathrm{T}}(x_i) \tag{15b}$$

where

$$\overline{W}_i(x)\equiv\overline{W}(x-x_i) \tag{16}$$

In equation (15a), matrix B has the form

$$B(x)=\left[B_1,B_2,...,B_n\right] \tag{17}$$

where

$$B_i=\overline{W}_i(x)\mathrm{p}(x_i) \tag{18}$$

and U_s is the vector that collects the nodal parameters of the field variables for all the nodes in the support domain

$$U_s=\{u_1,u_2,...,u_n\}^T \tag{19}$$

After solving equation (15a) for $\mathrm{a}(x)$, one gets

$$\mathrm{a}(x)=A^{-1}(x)B(x)U_s \tag{20}$$

Substitution of equation (11) at the above equation leads to

$$u^h(x)=\sum_{i=1}^{n}\sum_{j=1}^{m}\mathrm{p}_j(x)\left(A^{-1}(x)B(x)\right)_{ji}u_i \tag{21}$$

or

$$u^h(x)=\sum_{i=1}^{n}\Phi_i(x)u_i \tag{22}$$

where the Moving Least Square function $\Phi_i(x)$ is defined by

$$\Phi_i(x)=\sum_{j=1}^{m}\mathrm{p}_j(x)\left(A^{-1}(x)B(x)\right)_{ji}=\mathrm{p}^T A^{-1}B_i \tag{23}$$

We have to note that *m* is the number of the monomial terms of the polynomial basis p(x), and *n* is the number of nodes in the support domain, which is used for constructing the shape function. The requirement that $n>>m$ must be fulfilled for the moment matrix A to be invertible.

In order to obtain the spatial derivatives of the approximation function $u^h(x)$, it is necessary to obtain the derivatives of the MLS shape functions $\Phi(x)$.

$$\frac{\partial}{\partial x_i}u^h(x)=\frac{\partial}{\partial x_i}\sum_{i=1}^{n}\Phi_i(x)u_i=\sum_{i=1}^{n}\left\{\frac{\partial}{\partial x_i}\Phi_i(x)\right\}u_i \quad x_i=x,y,z \tag{24}$$

The derivative of the shape function is given as

$$\begin{aligned}\Phi_{i,x}(x)&=\left(\mathrm{p}^{\mathrm{T}}A^{-1}B_i\right)_{,x}=\\&=\mathrm{p}^{\mathrm{T}}_{,x}A^{-1}B_i+\mathrm{p}^{\mathrm{T}}\left(A^{-1}\right)_{,x}B_i+\mathrm{p}^T A^{-1}\left(B_i\right)_{,x}\end{aligned} \tag{25}$$

$$x_i=x,y,z$$

where $\left(A^{-1}\right)_{,x}=A^{-1}(x)A(x)A^{-1}(x)$ (26)

2.2 Weight Function Description

The weight function is non-zero over a small neighborhood of x_i, called the support domain of node i. The choice of the weight function $w(x-x_i)$ affects the resulting approximation $u^h(x_i)$ significantly. In the present paper a Gaussian weight function is used [Liu (2002)], yet the support domain does not have a standard point density value. Instead, a constant number of nodes are used for the approximation of the field function.

$$\overline{W}(x-x_i)\equiv\overline{W}(\overline{d})=\begin{Bmatrix}e^{-\left(\frac{\overline{d}_I}{a}\right)^2}\\0\end{Bmatrix} \tag{27}$$

where I=1, 2, 3, …, q are the nodes that produce the support domain of node x_i, and

$\overline{d}=\dfrac{|x-x_i|}{a_0^2}$ with a_0 a prescribed constant (often $a_0=0.3$) [**Error! Bookmark not defined.**].

3 Numerical Examples

3.1 Elliptic type: Poisson equation

In order to investigate the behavior of the constant nodal density support domain versus the constant nodal number support domain, we first examined a classical elliptic type PDE problem, Poisson equation with Dirichlet boundary conditions:

$$\begin{aligned}&\Delta u(x,y)=\left(x^2+y^2\right)e^{xy}, && \Omega=(0,1)\times(0,1)\\&u(x,y)=e^{xy}, && \partial\Omega\end{aligned} \tag{27}$$

The exact solution of this problem is the function e^{xy}. The above type form is known as the continuous problem (CP). A

unique solution exists if the criteria of the Theorem 6.13 in [Gilbarg and Trudinger (1983)] are fulfilled, i.e. if Ω is a bounded domain satisfying an exterior sphere condition at every boundary point and $f \in C^{s-2,a}(\Omega)$ for $s = 3,4$ and $u_p \in C(\partial\Omega)$. Then, the solution of the continuous problem is $u \in C^0(\overline{\Omega}) \cap C^{s,a}(\Omega)$, where $C^0(\overline{\Omega})$ is the vector space of all bounded and uniformly continuous functions on Ω, and $C^{s,a}(\Omega)$ represents the Holder space of exponent $0 < a < 1$ equipped with the norm

$$\|u\|_{C^{s,a}(\Omega)} \equiv \max_{0\le|\beta|\le s} \sup_{x\in\Omega} \left|D^\beta u(x)\right| + \max_{0\le|\beta|\le s} \sup_{x,y\in\Omega, x\neq y} \frac{\left|D^\beta u(x) - D^\beta u(y)\right|}{|x-y|^a} \quad (28)$$

In the present work, we solved the aforementioned Poisson equation numerically, using the strong form meshless point collocation method. Thus, the continuous problem had to be discretized. The field variable $u(x,y)$ was approximated with the MLS method described above, and the polynomial basis was of the second order, since Poisson equation is also a second order partial differential equation. Using the procedure described in [Kim and Liu (2006), Armentano and Durán (2001)] we formulated the discrete Poisson problem (DP)

$$(DP)\begin{Bmatrix} u_h \in V_g \equiv \{u_J \in \mathbb{R} \,|\, u_K = g(x_K) \text{ for all } x_K \in \Lambda^b\} \\ \Delta^p u^h = i(f), \quad \text{on } \Lambda^0 \end{Bmatrix} \quad (29)$$

with Δ^p being an operator called the ***strong meshfree Laplacian operator***, $\Lambda = \Lambda^0 \cup \Lambda^b$ are sets of well distributed interior and boundary nodes, respectively, and V_g is the finite dimensional space, subspace of $C(\overline{\Omega})$, of functions defined on Λ. The aforementioned procedure leads to a linear system of the unknown field variable. The system was solved with a direct method, providing the results for regular distributed 121 (Fig.1) and 441 (Fig.2) nodes given in the next section.

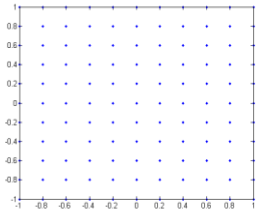

Fig.1. Grid of 121 regular distributed nodes

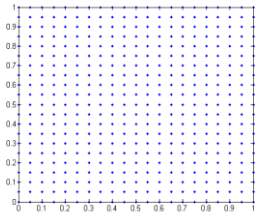

Fig.2. Grid of 441 regular distributed nodes

A crucial point concerning the meshfree methods is the domain representation. The latter is represented using sets of nodes distributed either regularly or irregularly, in its interior region and boundaries. The nodal distribution is usually not uniform and a denser distribution of nodes is often used in areas with high gradients or at discontinuities. Nevertheless, the discrete form of the above problem must converge in order to obtain a stable solution. Thus, the moment matrix $A(x) = \sum_{i=1}^{n} \overline{W_i}(x)\mathrm{p}(x)\mathrm{p}^{\mathrm{T}}(x_i)$ for the given set Λ of nodes must be invertible. To calculate the moment matrix and its inverse, one needs to focus on some class of node distributions. In the present work, we used the so-called Type I point distribution (i.e. staggered locally (p,4)-layered (p=2,3)) at each interior node, which is implemented on an open square domain. The second one used is of the Type II (i.e. locally (p,6)-layered (p=1,2)) at each interior node on a hexagonal domain (Fig.3).

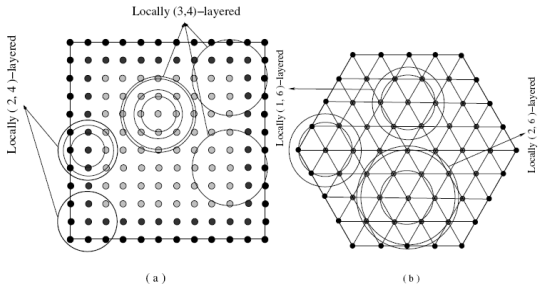

Fig.3. Possible layered node distributions [**Error! Bookmark not defined.**] (a) Type I (b) Type II

Each of these two distributions provides convergence and accuracy, since an error estimation analysis is obtained for the Poisson problem on the two specific domains [Kim and Liu (2006), Armentano and Durán (2001)].

The following Tables 1(a-b) and 2(a-b) show the accuracy of the numerical solution for the constant density and constant number support domain formulation using 121 and 441 regular distributed nodes.

Table 1a. Constant Density Support Domain for 121 total nodes

Support domain	Average number of nodes in SD	$\max(\lvert u^h - u_i \rvert)$	$\max(\lvert u_{exact} - u_h \rvert)$
2.0	121	$4.033\ 10^{+4}$	5.94
1.0	113	19	0.02
0.5	52	$1.99\ 10^{-3}$	$3\ 10^{-3}$
0.25	17	$1.274\ 10^{-4}$	$2.06\ 10^{-4}$
0.2	10	$2.065\ 10^{-5}$	$1.53\ 10^{-4}$
0.15	8	2.084	2.084
0.1	4	$7.73\ 10^{+6}$	$7.73\ 10^{+6}$

Table 1b. Constant Number Support Domain for 121 total nodes

Support domain	Average number of nodes in SD	$\max(\lvert u^h-u_i\rvert)$	$\max(\lvert u_{exact}-u_h\rvert)$
121	121	72	0.09
113	113	3.49	0.04
52	52	$7.19\ 10^{-3}$	$5.09\ 10^{-3}$
17	17	$4.31\ 10^{-4}$	$4.31\ 10^{-4}$
10	10	$5.60\ 10^{-5}$	$1.55\ 10^{-4}$
8	8	$2.29\ 10^{-5}$	$4.79\ 10^{-4}$
4	4	$7.73\ 10^{+6}$	$7.73\ 10^{+6}$

Table 2a. Constant Density Support Domain for 441 total nodes

SD	Average number of nodes in SD	$\max(\lvert u^h-u_i\rvert)$	$\max(\lvert u_{exact}-u_h\rvert)$
2.0	441	$5.47\ 10^{+7}$	5.94
1.0	422	$3.21\ 10^{+2}$	$9\ 10^{+2}$
0.5	200	0.25	$4\ 10^{-3}$
0.25	63	$3.02\ 10^{-4}$	$5.40\ 10^{-4}$
0.2	40	$1.46\ 10^{-4}$	$2.57\ 10^{-4}$
0.15	24	$4.97\ 10^{-5}$	$8.80\ 10^{-5}$
0.12	20	$1.39\ 10^{-5}$	$6.02\ 10^{-5}$
0.10	10	$5.89\ 10^{-6}$	$1.32\ 10^{-4}$
0.08	8	15.48	15.48

Table 2b. Constant Number Support Domain for 441 total nodes

number of nodes in SD	Average number of nodes in SD	$\max(\lvert u^h-u_i\rvert)$	$\max(\lvert u_{exact}-u_h\rvert)$
441	441	$2.73\ 10^{+10}$	$1.66\ 10^{+6}$
422	422	$1.86\ 10^{+11}$	$6.8\ 10^{+3}$
200	200	15.22	$42\ 10^{-3}$
63	63	$27.00\ 10^{-4}$	$13.45\ 10^{-4}$
40	40	$4.44\ 10^{-4}$	$4.45\ 10^{-4}$
10	10	$9.11\ 10^{-6}$	$1.40\ 10^{-4}$
8	8	$6.34\ 10^{-4}$	0.23

Clear trends in the local and global accuracies are evident in Tables 1 and 2, in view of the total number of nodes and the effect of the type of the support domain on the behavior of the solution. A lower cut-off in the magnitude of the support domain can be seen in the Tables, both for the 121 and the 441 total number of nodes cases, as proved by Kim and Liu (2006) and Armentano and Duran (2001) seems to be the optimum (minimum) number of nodes for the given node distribution type, Type I [Kim and Liu (2006)].

The improved behavior of the constant number of nodes formulation at low-numbered support domain cases can be noticed in the comparison of the accuracies in the results displayed at Tables 1 and 2. At average number of nodes 8, the constant number support domain formulation for 121 nodes, Table 1b, furnishes better results, that is, offers convergence i.e. stability. At the same conditions, the widely used constant density support domain formulation, shown in Table 1b, fails. The very same can be stated by direct comparison of Tables 2a and 2b (441 nodes) at average number of nodes 10, and at 8. Both the results shown at Tables 1(a-b) and the corresponding ones at Tables 2(a-b) can be used to claim the convergence to the Kronecker property for each nodal value in the present methodology by increasing the number of nodes in the domain Ω.

3.2 Parabolic type: Convection-Diffusion equation

Convection-diffusion problems are of great significance and very challenging in computational mechanics. However, only a handful of numerical methods are used to solve these kinds of problems. Examples are the widely used finite element method (FEM) and the closely related finite volume method (FVM). Nevertheless, significant problems had arisen using the aforementioned methods, which could be overcome by the so-called meshless methods. In particular, the Meshless Local Petrov-Galerkin (MLPG) method was used quite often to solve steady state convection-diffusion problems [Lin and Atluri (2000)]. The MLPG method is based on a weak form computed over a local sub-domain. As in FEM, the trial and test functions spaces can be different or the same, with Galerkin and Petrov-Galerkin upwinding, respectively. As far as the strong form of the convection-diffusion problems is used, very few works were reported [Gu and Liu (2006)]. However these techniques have faced several problems concerning the stability and the accuracy of the solution. The Reproducing Kernel Point Met (RKPM) Method, combined with the Streamline Upwind Petrov-Galerkin (SUPG) form of variational formulation was used in order to obtain more accurate results [Onate, Idelsohn, Zienkiewicz, and Taylor (1996)]. The stability problem is discussed in the analysis of the convection dominated problems using meshfree methods in [Gu and Liu (2006)]. Several techniques are proposed, including the enlargement of the support domain, the upwinding support domain, the adaptive upwinding support domain and the nodal refinement. The meshless point collocation method is used for discretization, and radial basis functions are used to approximate the unknown field variable [Sarler (2005), Mai-Cao and Tran-Cong (2005), Mai-Duy (2004)]. All the above techniques are developed in order to overcome the stability and accuracy problems, and the final goal is the enhancement of the accuracy for high gradient problems. Particularly for problems dominated by high regularities at the boundaries, such as high gradients, the weak form is usually preferred instead of the strong form. In this paper we try to solve the 1D and 2D convection-diffusion problem using meshless point collocation method with Moving Least Square (MLS) approximation. We use a constant number support domain for the weight function, and

we propose a fully automated nodal refining procedure based on theorems proved in Kim and Liu (2006) and Armentano and Duran (2001). The upwind method provides stable and accurate results with a very clear physical meaning. Nevertheless, to the authors' attention, the upwind method lacks of a pure mathematical convergence and stability analysis, as far as the meshless methods are concerned. Thus, we used a strong mathematical proof for defining the concept of well distributed nodes, and implemented it for nodal refinement at nodes where the absolute value of the ***strong form error*** $R=\left|Lu^h(x,y)-f\right|$ is larger than a user defined threshold (e.g. $R<10^{-2}$).

3.3 1D Convection-Diffusion

In this section a one-dimensional (1-D), steady-state, convection-diffusion problem is considered. The governing equation is:

$$V\frac{du}{dx}-\frac{d}{dx}\left(D_m\frac{du}{dx}\right)+q=0, \qquad x\in(0,1) \tag{30a}$$

where u is the field scalar variable, V, D_m, q are all given constants, having different physical meaning for each engineering problem.

The following Dirichlet boundary conditions are considered:

$$\begin{aligned} u|_{x=0}&=0\\ u|_{x=1}&=1 \end{aligned} \tag{30b}$$

The exact solution for this problem can be easily obtained by solving this second order ordinary differential equation (ODE), with essential boundary conditions, analytically. It is well known that the stability of the numerical solution of the above problem is defined by a number, called the Peclet (Pe) number:

$$Pe=\frac{Vd_s}{2D_m} \tag{31}$$

with d_s being the nodal spacing for two neighbor nodes. It has been shown [Gu and Liu (2006)] that, when Pe is very large $(Vd_s\gg D_m)$, Eq. (30a-b) becomes convection-dominated, and the accuracy of the standard numerical results becomes oscillatory. The second term in the equation becomes negligible, resulting in that the boundary condition $u|_{x=1}=1$ affects only a very narrow region of the domain. Thus, a thin boundary layer is formed causing stability problems to the obtained numerical solution. These stability problems make the thin boundary layer difficult to be reproduced (resulting in an oscillatory unstable solution) by the standard numerical methods if no special care is considered. This kind of instability can occur in many numerical methods, such as FEM, FVM, FDM and meshfree methods. In order to overcome this problem, the upstream information of the field variable approximation has to be prescribed with great accuracy. Several strategies for meshless methods were developed, such as nodal refinement, enlargement of the local support domain, fully upwind support domain, and adaptive upwind support domain [Gu and Liu (2006)]. All the aforementioned methods have several advantages and disadvantages. For nodal refinement, the increase at the number of nodes decreases the nodal spacing d_s and the Peclet number, although there is an increase in computational time. By enlarging the local support domain one captures the upstream information but reduces the accuracy of the solution [Liu (2002)]. This can be more evident when regions with high gradients are present. By using an upwind support domain, the accuracy and stability is improved for problems with high Peclet number, still it gives very poor results for smaller Peclet numbers. Using constant number support domain obtained a solution with inaccuracies for 40 regular distributed nodes, as it is clear at (Fig.4).

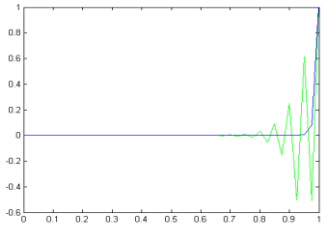

Fig.4 Exact solution (blue line) and numerical solution

By defining the nodes with a strong error value greater than a defined threshold (Fig.5), a local refined is implemented providing the solution at (Fig.6)

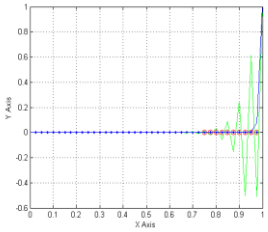

Fig.5 Red spots: Nodes for refinement

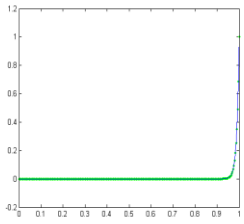

Fig.6 Exact and numerical solution (green spots)

with $\max\left|u_{num}-u_{exact}\right|=0.02$

3.4 2D Convection-Diffusion

We next consider the two-dimensional convection-diffusion equation

$$-\varepsilon\nabla^2u+\vec{w}\nabla u=f \tag{32}$$

where $\varepsilon > 0$. The above equations arise in numerous models of flows and other physical phenomena. The unknown field function u may represent the concentration of a polymer being transported (or 'convected') along a stream moving at velocity $\vec{w}$ and subject to diffusive effects. It also may represent the temperature of a fluid moving along a heated wall, or the concentration of electrons in models of semiconductor devices. Typically, diffusion has less significant physical effect, compared to convection. Thus, for most practical problems, $\varepsilon \ll |\vec{w}|$. As it is well known, a boundary layer is formed when the convection term is dominated. The crucial point for a numerical method is to describe the very boundary layer with accuracy. In this work, we solve a convection-diffusion problem on a square domain $\Omega = (-1,1)\times(-1,1)$ with source term $f = 0$ and $\varepsilon = \frac{1}{200} \ll 1$. Since the Peclet number is inversely proportional to ε, the problem is convection dominated. The velocity $\vec{w}$ is constant with $\vec{w} = (0,1)$ and the Dirichlet boundary conditions are:

$$u(x,-1) = x, \quad u(x,1) = 0$$
$$u(-1,y) \approx -1, \; u(1,y) \approx 1 \qquad (33)$$

where the latter two approximations hold everywhere in the domain except near $y = 1$. On the boundaries $x = \pm 1$ the boundary values vary dramatically near $y = 1$, changing from (essentially) -1 to 0 on the left and from +1 to 0 to the right. For small ε, the solution u is very close to that of the reduced problem $u^h \equiv x$ except near the outflow boundary $y = 1$, where it is zero. This dramatic change constitutes a boundary layer. The exact solution of the problem is

$$u(x,y) = x\left(\frac{1 - e^{\frac{y-1}{\varepsilon}}}{1 - e^{\frac{-2}{\varepsilon}}}\right) \qquad (34)$$

A solution is obtained for a regular grid 11x11 (Fig.7).

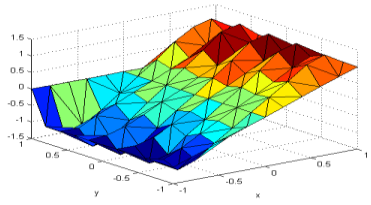

Fig.7 Numerical solution for 121 nodes

By calculating the absolute value of the strong form error $|Lu - f|$ we point out the nodes with values greater than a user defined threshold value $\theta = 0.01$ (Fig.8).

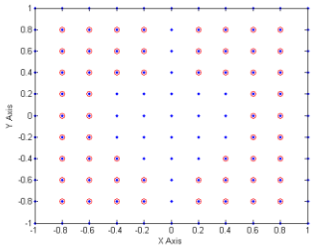

Fig. 8 Nodes for local refinement

It follows the refinement of the nodes by using a rectangular orientation of the added nodes surrounding the prescribed nodes (Fig.9).

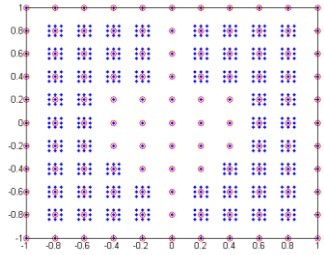

Fig.9 Node distribution after refinement

Finally, the new solution is calculated and the errors are estimated (Fig.10).

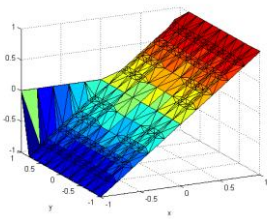

Fig10 Solution of the refined nodes

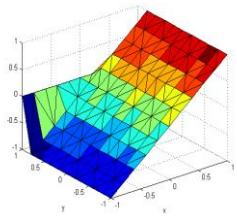

Fig.11 Exact solution

The strong form errors are presented. First in (Fig.12) the errors before the refinement are plotted and then those after the refinement (Fig.13), showing the error decreasing and the greater accuracy for the numerical solution. The prescribed procedure is fully automated, giving the opportunity for following refinements until the desirable accuracy (e.g R<0.0001) is obtained.

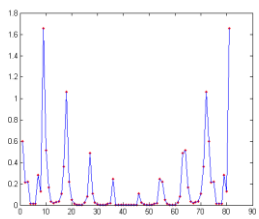

Fig.12 Strong Error before refinement

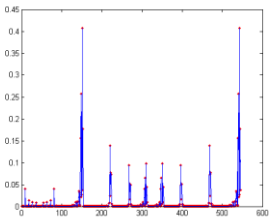

Fig.13 Strong Error after refinement

3.5 2D Steady State Stokes Equations

The Stokes equation system

$$-\nu.\nabla^2\vec{u}+\nabla p=\vec{f}$$
$$\nabla\vec{u}=0 \qquad (35)$$

is a fundamental model of viscous incompressible flow. The variable $\vec{u}$ is a vector-valued function representing the velocity of the fluid, and the scalar function p represents the pressure. The first equation represents the conservation of the momentum of the fluid (momentum equation), whereas the second one enforces conservation of mass. The crucial modelling assumption made is that the flow is "low-speed", so that convection effects can be neglected. Such flows arise in cases where the fluid is very viscous or where it is tightly confined. An example is the flow of blood in parts of the human body. For the purpose of our study we choose to solve the 2D flow of a fluid passing a stenosed region (Fig.14) with Dirichlet boundary conditions. The length at the inlet and outlet region is 0.6 mm and the point of the stenosis the length is 0.2 mm. The distance L of the central axis is 1 mm. The dynamic viscosity μ is 1 cP and the density ρ is 1 kg/m^3 (Stokes conditions). The pressure difference is the driving force for the fluid flow, with pressure set to 1 kPa at the left entrance, and 0 kPa at the right one. The gravity is neglected, thus $f=0$.

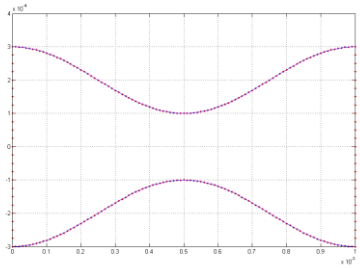

Fig.14 Stenosed 2D region geometry

The unknown field approximation was implemented with the MLS method and the discretization scheme is the meshless point collocation method. For each node the degrees of freedom are three, the two velocity components u_x and u_y, and the pressure value p. The differential operator $L\equiv\nabla^2+\nabla$ is an elliptical type operator and thus, the maximum principle method implies that this operator should converge when used with meshless point collocation method and well-distributed nodes [Kim and Liu (2006)]. The nodal distribution used is a regular one (Fig.15) of Type I, as already pointed out, so that the moment matrix A is invertible.

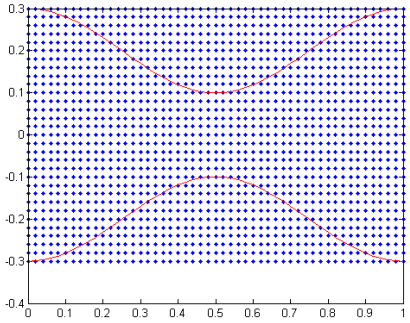

Fig.15 Regular node distribution at a bounding box of the geometry

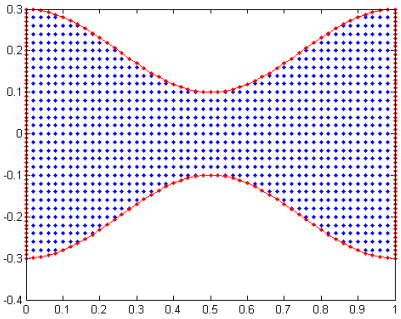

Fig.16 Final node distribution. Blue nodes are the interior nodes

A comparison took place between the solution obtained and the solution provided by the finite element method. The latter implemented with the commercial software package ANSYS CFX 5.1. Results are shown in Figs.17-19.

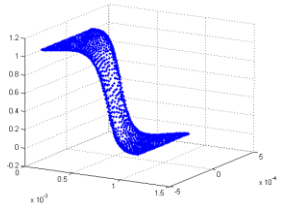

Fig.17a ANSYS pressure plot

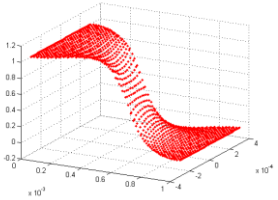

Fig.17b Meshless pressure plot

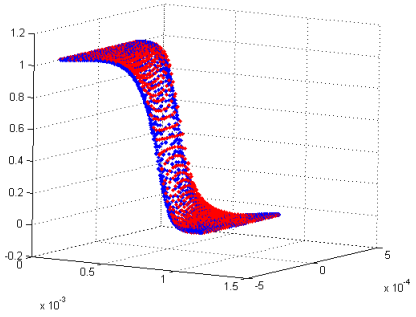

Fig.17c ANSYS-Meshless pressure plot

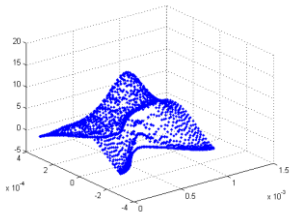

Fig.18a ANSYS [u] velocity plot

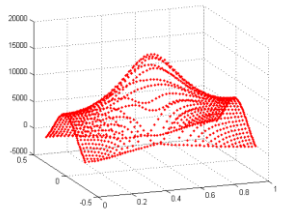

Fig.18b Meshless [u] velocity plot

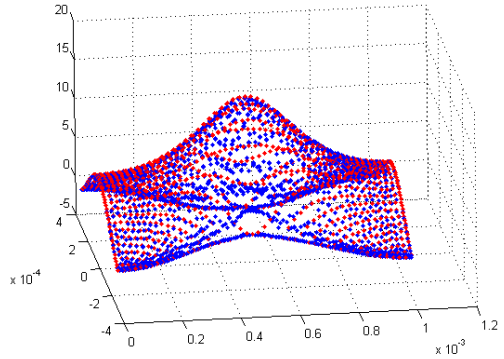

Fig.18c ANSYS-Meshless [u] velocity plot

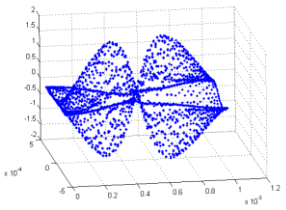

Fig.19a ANSYS [v] velocity plot

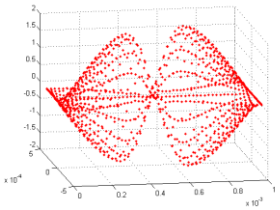

Fig.19b Meshless [v] velocity plot

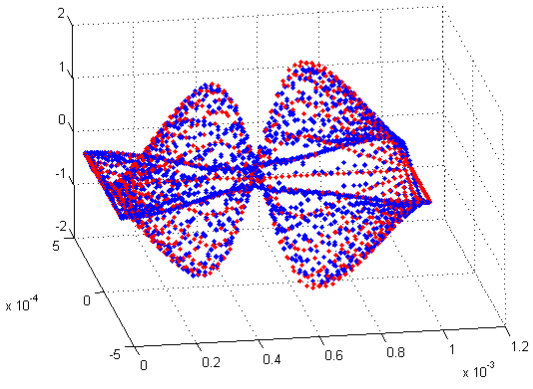

Fig.19c ANSYS-Meshless [v] velocity plot

4 Discussion

In the present work we restrict our study to numerical methods that can solve partial differential equations problems without integration. This implies that we ignore boundary integral equation methods and finite elements, and insist on truly meshless methods. Thus, the MLS approximation was used herein of the construction of the trial functions during a strong-form description of several physical problems. To the authors' attention, this is one of the few attempts for unknown function approximation with the meshless collocation technique. We examined the behavior of the solution with regular and irregular node distribution, combined with either constant density or constant number support domain, by the implementation of the collocation method at elliptic type (Poisson equation) partial differential equations. As it has been proved with the maximum principle method [Kim and Liu (2006)], the Laplacian operator of the elliptic problem converges. The accuracy is increased using greater number of nodes, and using constant number of nodes for the support domain. It has also pointed out [Armentano and Durán (2001)] that a well-distributed set of nodes should be used, in order to obtain a stable solution.

The constant number technique for convection-diffusion problems was used for parabolic type of partial differential equations, during the evaluation of the support domain for the construction of the approximation function. The improved behavior of the constant number of nodes formulation, proposed in the present work, furnishes more stable results at the low-numbered (optimum) support domain cases, where the widely used constant density support domain formulation occasionally fails.

A fully automated procedure was developed, based on the error of the strong form description evaluation for the nodal refinement while keeping the well-distribution of nodes, provided a solution with great stability and accuracy, reducing the overall computational cost of a global refinement. Finally, it is has been shown [Ciarlet and Raviart (1973)] that the existence of a maximum principle for the discrete problem implies the possibility of obtaining uniform convergence of the approximates solutions to the exact solutions, for three of the most popular approximation schemes for solving second order Dirichlet problems, i.e., classical finite differences, variational finite differences, and finite element methods. A mathematical background has been developed recently for the convergence [Kim and Liu (2006)] and for the error bounds [Armentano and Durán (2001)] of meshless collocation methods. One can use this method for elliptic and parabolic type of problems, in conjunction with smart refinement techniques, as the one proposed in this paper. Proof of the above hypothesis has been shown for (at least) elliptic type of operators (Laplacian) and for MLS trial functions.

Future work involves the mathematical treatment and the implementation of the Neumann type boundary conditions. Also, the convergence analysis for nodal distribution has to be extended to irregular geometries for 2D and 3D space dimensions. As far as problems with Stokes flow are concerned, comparison of the results of the meshless PC method using MLS approximation with the results obtained by ordinary FE methods indicates that the two methods are

directly comparable both in accuracy, and in computational time. However, a strict mathematical proof of the PCM performance in Stokes flow problems has still to be examined. Strong form of PDEs provides the "complete" solution of the problem, a solution that is both unique and stable. For elliptic type of problems, MLS discrete strong form point collocation methods can nowadays be used with sufficient accuracy and stability, in order to be applied in coupled, multiphase and/or multiscale problems.

5 Acknowledgments

The authors would like to acknowledge University of Patras Research Committee (K. Karatheodoris program) for financial support.

References

Aktas, O.; Aluru, N. R. (2002): A combined continuum/ DSMC technique for multiscale analysis of microfluidic filters. *J Comp Phys*, vol. 178, pp. 342-372.

Armentano, M. G.; Durán R. G. (2001): Error estimates for moving least square approximations. *Appl Numer Math*, vol 37, pp. 397-416.

Atluri, S. N. (2004): *The Meshless Method (MLPG) for Domain & BIE Discretization*, Tech Science Press.

Atluri, S. N.; Shen, S. (2002): The Meshless Local Petrov-Galerkin (MLPG) Method, 440 pages, Tech Science Press

Atluri, S. N.; Sladek, J.; Sladek V.; Zhu, T. (2000): The Local boundary integral equation (LBIE) and it's meshless implementation for linear elasticity. *Comput Mech*, vol. 25, pp. 180-198.

Atluri, S. N.; Zhu, T. (1998): A new meshless local Petrov-Galerkin (MLPG) approach in computational mechanics. *Comput Mech*, vol. 22, pp. 117-127.

Atluri, S. N., **Liu, H. T.**, **Han, Z. D.** (2006): Meshless Local Petrov-Galerkin (MLPG) Mixed Finite Difference Method for Solid Mechanics, *CMES-Comp Model Eng Sci*, vol. 15 (1), pp. 1-16

Belytschko, T.; Lu, Y.Y.; Gu, L. (1994): Element free Galerkin methods. *Int J Numer Meth Eng*, vol. 37, pp. 229-256.

Burganos, V. N.; Skouras, E. D.; Paraskeva, C. A.; Payatakes, A. C. (2001): Simulation of the dynamics of depth filtration of non-Brownian particles, *AIChE J*, vol 47 (4), pp. 880-894.

Ciarlet P. G.; Raviart, **P. A.** (1973): Maximum Principle and Convergence for the Finite Element Method, *Comput Meth Appl Mech Engng*, vol 2, pp.17-31.

Garcia, A. L.; Bell, J. B.; Crutchfield, W. Y.; Alder, B.J. (1999): Adaptive Mesh and Algorithm Refinement Using Direct Simulation Monte Carlo. *J. Chem. Phys.*, vol. 154, pp. 134-155.

Gilbarg, D.; Trudinger, N. S. (1983): *Elliptic Partial Differential Equations of Second Order*, 2nd ed., Springer, New York.

Gingold, R. A.; Monaghan, J. J. (1977): Smoothed particle hydrodynamics: theory and applications to non-spherical stars. *Mon Not R Astron Soc*, vol. 181, pp. 375-389.

Gu, Y. T.; Liu, G. R. (2006): Meshless techniques for convection dominated problems. *Comp Mech*, vol. 38, pp. 171-182.

Han, Z. D.; Liu, H. T.; Rajendran, A. M.; Atluri, S. N. (2006): The Applications of Meshless Local Petrov-Galerkin (MLPG) Approaches in High-Speed Impact, Penetration and Perforation Problems, *CMES-Comp Model Eng Sci*, vol. 14(2), pp. 119-128

Kagadis, G. C.; Skouras, E. D.; Bourantas, G. C.; Paraskeva, C. A.; Katsanos, K.; Karnabatidis, D.; Nikiforidis, G. C. (in press): Computational Representation of In-Vivo Acquired Stenotic Renal Artery Geometries Using Turbulence Modeling, *Med Eng Phys*.

Kim D. W.; Liu W. K. (2006): Maximum principle and convergence analysis for the meshfree point collocation method. *Siam J Numer Anal*, vol. 44 (2), pp. 515-539.

Lin, H.; Atluri, S. N. (2000): Meshless local Petrov-Galerkin (MLPG) method for convection-diffusion problems. *CMES-Comp Model Eng Sci*, vol. 1 (2), pp. 45-60.

Liszka, T. J.; Duarte, C. A. M.; Tworzydlo, W. W. (1996): Hp-meshless cloud method. *Comput Method Appl M*, vol. 139, pp. 263-288.

Liu, W.K.; Jun, S.; Sihling, D.T.; Chen, Y.; Hao, W. (1997): Multiresolution reproducing kernel particle method for computational fluid mechanics., *Int J Numer Meth Fl*, vol. 20, pp. 1081-1106.

Liu, G.R. (2002): *Mesh Free Methods, Moving beyond the Finite Element Method*, CRC Press.

Liu, W. K.; Chen, Y.; Jun, S.; Chen J. S.; Belytschko, T., Pan, C.; Uras, R. A.; Chang, C. T. (1996): Overview and applications of the reproducing kernel particle methods. *Arch Comput Method E*, vol. 3, pp. 3-80.

Mai-Cao, L.; Tran-Cong, T. (2005): A Meshless IRBFN-based Method for Transient Problems, *CMES-Comp Model Eng Sci*, vol. 7 (2), pp. 149-172.

Mai-Duy, N. (2004): Indirect RBFN Method with Scattered Points for Numerical Solution of PDEs, *CMES-Comp Model Eng Sci*, vol. 6 (2), pp. 209-226.

Michalis, V. K.; Kalarakis, A. N.; Skouras, E. D.; Burganos, V. N. (2008): Mesoscopic Modeling of Flow and Dispersion Phenomena in Fractured Solids. *Comput Math Appl*, vol. 55 (7), pp. 1525-1540.

Navascués, N.; Skouras, E. D.; Nikolakis, V.; Burganos, V. N.; Tellez, C.; Coronas, J. (in press): Re-construction of umbite framework variants by atomistic simulations using XRD and sorption data. *Chem Eng Proc*.

Nayroles, B.; Touzot, G.; Villon, P. (1992): Generalizing the finite element method: diffuse approximation and diffuse elements. *Comput Mech*, vol. 10, pp. 307-318.

Onate, E.; Idelsohn, S.; Zienkiewicz, O. C.; Taylor, R. L. (1996): A finite point method in computational mechanics. Application to convective transport and fluid flow. *Int J Num Meth Eng*, vol. 39, pp. 3839-3866.

Sarler, B. (2005): A Radial Basis Function Collocation Approach in Computational Fluid Dynamics, *CMES-Comp Model Eng Sci*, vol. 7 (2), pp. 185-194.

Schaback, R. (2007): Convergence of unsymmetric kernel-based meshless collocation methods, *Siam J Numer Anal*, vol. 45 (1), pp. 333-351.

Skouras, E. D.; Paraskeva, C. A. ; Burganos, V. N.; Payatakes, A. C. (2007): Simulation of the Dynamic Behavior of Horizontal Granular Filters, *Sep Purif Technol*, vol. 56, pp. 325.